Bioconjugate Chemistry

Article

pubs.acs.org/bc

New Bifunctional Chelator for ^{64}Cu-Immuno-Positron Emission Tomography

Darpan N. Pandya,[†] Nikunj Bhatt,[†] Ajit V. Dale,[†] Jung Young Kim,[‡] Hochun Lee,[§] Yeong Su Ha,[†] Ji-Eun Lee,[∥] Gwang Il An,[‡] and Jeongsoo Yoo*,[†]

[†]Department of Molecular Medicine, Kyungpook National University, Daegu 700-422, South Korea

[‡]Molecular Imaging Research Center, Korea Institute of Radiological and Medical Sciences, Seoul 139-706, South Korea

[§]Department of Energy Systems Engineering, Daegu Gyeongbuk Institute of Science & Technology, Daegu, 711-873, South Korea

[∥]Central Instrument Facility, Gyeongsang National University, Jinju, 660-701, South Korea

Supporting Information

ABSTRACT: A new tetraazamacrocyclic bifunctional chelator, TE2A-Bn-NCS, was synthesized in high overall yield from cyclam. An extra functional group (NCS) was introduced to the *N*-atom of TE2A for specific conjugation with antibody. The Cu complex of TE2A-Bn-NCS showed high kinetic stability in acidic decomplexation and cyclic voltammetry studies. X-ray structure determination of the Cu-TE2A-Bn-NH_2 complex confirmed octahedral geometry, in which copper atom is strongly coordinated by four macrocyclic nitrogens in equatorial positions and two carboxylate oxygen atoms occupy the elongated axial positions. Trastuzumab was conjugated with TE2A-Bn-NCS and then radiolabeled with ^{64}Cu quantitatively at room temperature within 10 min. Biodistribution studies showed that the ^{64}Cu-labeled TE2A-Bn-NCS-trastuzumab conjugates maintain high stability in physiological conditions, and NIH3T6.7 tumors were clearly visualized up to 3 days by ^{64}Cu-immuno-positron emission tomography imaging in animal models.

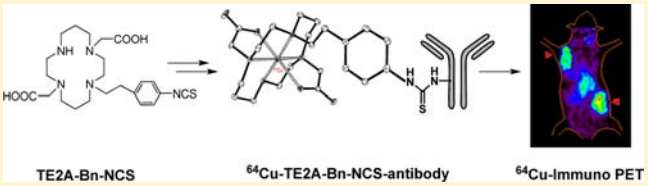

INTRODUCTION

Recent advances in antibody technologies has made it feasible to develop antibodies having high specific binding for essentially any molecular target of interest.[1,2] To date several dozen monoclonal antibodies (mAbs) have been approved by U.S. Food and Drug Administration (FDA) for use as diagnostics[3] and therapeutics[4] in various medical indications.[5,6] Furthermore, hundreds of new mAbs and engineered mAb fragments (i.e., diabody, minibody, single chain variable fragment, and nanobody) are at stages of early clinical trial and preclinical evaluation.

Immuno-positron emission tomography (immuno-PET) is the most powerful imaging tool for the tracking and quantification of antibodies in vivo because PET can provide noninvasive, quantitative assessment of molecular events in the whole body at high spatial resolution and sensitivity.[7,8] The information obtained by immuno-PET is crucial in most stages of antibody-based drug development and ultimately for personalized imaging and therapy.[2,6]

For immuno-PET imaging, mAbs and engineered mAb fragments need to be radiolabeled with radioisotopes emitting positron (β^+) such as ^{68}Ga ($t_{1/2}$ = 68 min), ^{18}F ($t_{1/2}$ = 110 min), ^{64}Cu ($t_{1/2}$ = 12.7 h), ^{86}Y ($t_{1/2}$ = 14.7 h), ^{76}Br($t_{1/2}$ = 16.2 h), ^{89}Zr ($t_{1/2}$ = 78.4 h), and ^{124}I ($t_{1/2}$ = 100.2 h).[8] Among these isotopes, Cu-64 is of special interest because of its midlong half-life as well as its attractive decay modes (β^- 39%, β^+ 17%).[9] In addition, Cu-64 can be routinely produced in large quantity and high specific activity using a biomedical cyclotron.[10]

However, the radiolabeling of antibody with Cu-64 is not simple but needs more sophisticated considerations compared to small biomolecules (e.g., peptide, aptamer). Due to intrinsic fragility of antibody to heat and radiation, the radiolabeling step should proceed at mild conditions: ambient temperature, narrow pH range, and short labeling time.[11,12] In most cases, antibody is not radiolabeled directly with Cu-64, but instead is conjugated with bifunctional chelator (BFC) first, and then the BFC−antibody conjugate is radiolabeled with radioactive copper ions via BFC.[13,14] The ^{64}Cu-radiolabeled antibody should maintain high in vivo stability for accurate PET imaging and the decomplexation of ^{64}Cu ion from BFC should be minimized until imaging time point. However, most antibodies have much longer blood half-life compared to small molecules, and usually 1−2 days are taken to reach optimal target-to-background ratio for monoclonal antibody imaging. This is why higher robustness of Cu-BFC complex is needed for successful ^{64}Cu-immunoPET imaging.

So far, tetraazamacrocyclic BFCs such as DOTA (1,4,7,10-tetraazacyclododecane-*N*,*N*′,*N*″,*N*‴-tetraacetic acid) and TETA (1,4,8,11-tetraazacyclotetradecane-*N*,*N*′,*N*″,*N*‴-tetraacetic acid)

Received: April 17, 2013
Revised: July 24, 2013
Published: July 24, 2013

 © 2013 American Chemical Society dx.doi.org/10.1021/bc400192a | *Bioconjugate Chem.* 2013, 24, 1356−1366

have been commonly used to radiolabel antibodies with ^{64}Cu ions because they have several advantages, i.e., easy availability, high radiolabeling yield at reasonable temperature (<40 °C), and higher Cu(II) complex stability than acyclic chelators such as EDTA and DTPA.[15−18] However, recent studies showed that the Cu complexes of these BFCs slowly lose Cu(II) ions in vivo, which results in an increase in unnecessary radiation exposure to nontargeting organs and background noise in imaging.[19,20] For more specific conjugation with antibody, new DOTA and TETA derivatives having an extra functional group (e.g., NH_2, NCS) on carbon backbone or *N*-atom of macrocycles were synthesized (Figure 1).[21−24] However, such

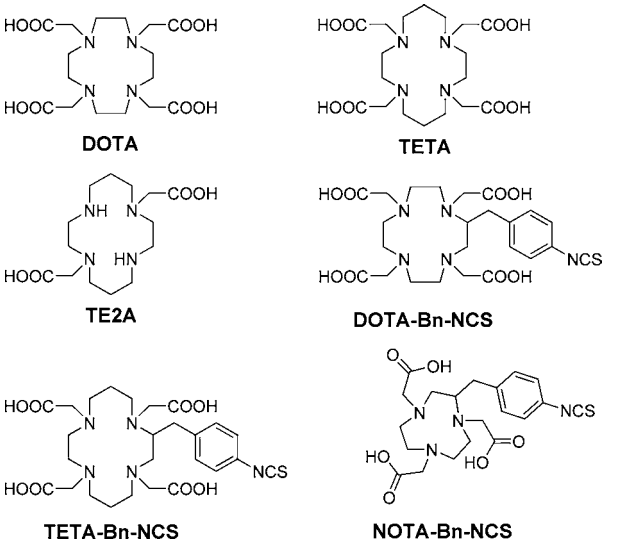

Figure 1. Typical azamacrocyle-based bifunctional chelators for antibody labeling.

sophisticated BFCs can only be obtained via multiple-step synthesis leading to a very low overall yield. Furthermore, because those BFCs are still based on DOTA or TETA backbone, the complex stability issue was left unsolved.

In order to address the in vivo stability issue of Cu-BFC complexes, new types of BFCs were developed. Anderson and colleagues reported that cross-bridged TE2A formed extremely stable Cu complexes and the release of free ^{64}Cu ions is minimized in physiological condition.[20,25] However, these cross-bridged chelators can be radiolabeled at only high temperature and cannot be used for radiolabeling of heat-sensitive antibodies.[26] Very recently, the same group reported that phosphate analogs of cross-bridged TE2A can be radiolabeled at milder conditions, but the radiolabeled antibody using new chelators has not been reported yet.[27,28]

Recently, we reported that TE2A (1,8-*N*,*N*′-bis-(carboxymethyl)-1,4,8,11-tetraazacyclotetradecane) is a potentially better bifunctional chelator than widely used TETA in terms of higher kinetic stability and quantitative radiolabeling at room temperature.[29] TE2A can be utilized as a BFC in the same way as TETA by conjugating TE2A with antibody using one of two acetic acid pendant arms.[30] However, TE2A itself contain two reactive secondary amine groups which can compete with the amine group of the antibody in the conjugation reaction. Furthermore, upon conjugation one of its acetic acid pendant arms should be consumed for conjugation and will not be available for strong coordination bonding to Cu(II) ion.[31] In addition to these conjugation problems, the overall charge of the formed Cu-TE2A conjugate is also changed from neutral to +1. However, it is well-known that the positively charged Cu complexes show higher uptake in clearance organs such as liver and kidney and the body clearance is retarded compared to that of neutral complexes.[32,33] Of course, the effect of charge change of Cu-TE2A conjugate will be minimal when TE2A is conjugated with large monoclonal antibody. However, the same charge change may have significant influence on its physiological behavior when conjugated with small antibody fragments or even smaller peptides.

Trastuzumab, most commonly known as Herceptin (Genetech, Inc.), is the first FDA-approved humanized recombinant monoclonal antibody to target solid tumor.[34] It binds to the extracellular domain of the HER2 receptor and inhibits the proliferation and survival of HER2-dependent tumors. Trastuzumab has been used more than 10 years for the treatment of metastatic breast cancer showing high over-expression of the HER2 protein.[35] Fibroblast NIH3T6.7 cell, which is a HER2 overexpressing NIH3T3 cell line, has been widely used in HER2 targeting studies.[36−38]

Here we present a new TE2A derivative (TE2A-Bn-NCS) in which an extra isothiocyanate group is introduced on one of two secondary amines for facile conjugation with antibody while maintaining high kinetic stability of the neutral Cu-TE2A complex. TE2A-Bn-NCS is conjugated with a monoclonal antibody (trastuzumab) through the NCS functionality of BFC. The in vivo stability and targeting affinity of ^{64}Cu-labeled TE2A-Bn-NCS-trastuzumab are examined in Her2/neu positive tumor models. New TE2A-Bn-NCS chelator shows very promising properties as a BFC for ^{64}Cu-immuno-PET imaging.

■ EXPERIMENTAL SECTION

Materials and Reagents. Cyclam and DOTA-Bn-NCS were purchased from CheMatech (Dijon, France) and Macrocyclics (Dallas, USA), respectively. All other reagents and solvents were purchased from Sigma-Aldrich (St. Louis, MO) and were used as received. Copper-64 was produced at KIRAMS (Seoul, Korea) by the ^{64}Ni(p,n)^{64}Cu nuclear reaction using an MC50 Cyclotron (Scanditronix, Sweden).

Synthesis of 1,8-*N*,*N*′-Bis-(carbo-*tert*-butoxymethyl)-1,4,8,11-tetraazacyclotetradecane (4). A 3 M NaOH solution (200 mL) was added to **3** (9.15 g, 14.89 mmol). After stirring for 3 h, the resultant solution was extracted with $CHCl_3$ (3 × 100 mL), the combined organic phases were washed by brine, dried over $MgSO_4$, and solvent was evaporated under reduced pressure to give an oil **4** (6.25 g, 98% yield) which solidified on standing. ^{1}H NMR (500 MHz, $CDCl_3$, 25 °C): δ = 1.37 (s, 18H; CH_3), 1.69−1.71 (m, 4H; CH_2), 2.72−2.59 (m, 16H; CH_2), 3.25 (s, 4H; CH_2); ^{13}C NMR (125 MHz, $CDCl_3$, 25 °C): δ = 25.78, 28.09, 47.59, 50.02, 52.47, 54.13, 54.74, 80.57, 170.43; HRMS (FAB) calculated for $C_{22}H_{45}N_4O_4$, 429.3441 $[M+H]^+$, found: 429.3439 $[M+H]^+$.

Synthesis of 1,8-*N*,*N*′-Bis-(carbo-*tert*-butoxymethyl)-4-*N*″-(4′-nitrophenethyl)-1,4,8,11-tetraazacyclotetradecane (5). A mixture of 1,8-*N*,*N*′-bis-(carbo-*tert*-butoxymethyl)-1,4, 8,11-tetraazacyclotetradecane **4** (3.28 g, 7.65 mmol), 4-nitrophenethyl bromide (5.28 g, 22.96 mmol), anhydrous K_2CO_3 (5.29 g, 38.26 mmol), and KI (1.27 g, 7.65 mmol) in anhydrous toluene (150 mL) was refluxed for 1 day. The solvent was evaporated from reaction mixture under reduced pressure and CH_2Cl_2 (250 mL) was added. The resulting brown slurry was filtered off through a Celite pad and washed

dx.doi.org/10.1021/bc400192a | *Bioconjugate Chem.* 2013, 24, 1356−1366

with CH_2Cl_2 (2 × 30 mL). The combined filtrate and washings were evaporated under reduced pressure. The resulting residue was purified via column chromatography on alumina (basic), eluting with EtOAc/methanol (5:1) to afford a yellow oil **5** (3.02 g, 68% yield). ^{1}H NMR (500 MHz, $CDCl_3$, 25 °C): δ = 1.38−1.40 (d, $^2J_{(H,H)}$ = 10 Hz, 18H; CH_3), 1.62 (br s, 2H; CH_2), 1.88 (br s, 2H; CH_2), 2.51−2.71 (m, 12H; CH_2), 2.82−2.88 (m, 4H; CH_2), 2.97 (br s, 4H; CH_2), 3.20−3.23 (d, $^2J_{(H,H)}$ = 15 Hz, 4H; CH_2), 7.33−7.35 (dd, $^2J_{(H,H)}$ = 10 Hz, 2H; CH), 8.06−8.08 (dd, $^2J_{(H,H)}$ = 10 Hz, 2H, CH); ^{13}C NMR (125.8 MHz, $CDCl_3$, 25 °C): δ = 23.24, 24.41, 28.13, 28.14, 31.98, 46.12, 48.37, 49.57, 50.02, 52.05, 52.51, 53.18, 55.02, 55.36, 55.67, 81.08, 81.36, 123.54, 129.57, 146.33, 148.62, 170.49, 170.70; HRMS (FAB) calculated for $C_{30}H_{52}N_5O_6$, 578.3918 $[M+H]^+$, found: 578.3915 $[M+H]^+$.

Synthesis of 1,8-*N,N′*-Bis-(carboxymethyl)-4-*N″*-(4′-nitrophenethyl)-1,4,8,11-tetraaza cyclotetradecane (6·2TFA). Compound **5** (1.35 g, 2.34 mmol) was dissolved in a 1:1 (v/v) mixture of CF_3CO_2H (TFA) and CH_2Cl_2 (72 mL). The mixture was stirred at room temperature for 24 h. The solvent was removed under reduced pressure to give an oily residue which was triturated in Et_2O to provide off-white solid **6** as a TFA salt (1.57 g, 97% yield). ^{1}H NMR (500 MHz, D_2O, 25 °C): δ = 1.80−2.10 (m, 4H; CH_2), 2.61−2.90 (m, 6H; CH_2), 2.92−3.81 (m, 18H; CH_2), 7.46−7.48 (dd, $^2J_{(H,H)}$ = 10 Hz, 2H; CH), 8.10−8.12 (dd, $^2J_{(H,H)}$ = 10 Hz, 2H; CH); ^{13}C NMR (125.8 MHz, D_2O, 25 °C): δ = 21.34, 22.77, 28.16, 45.02, 47.60, 50.14, 50.38, 51.46, 51.67, 53.13, 54.23, 54.58, 56.22, 116.43 (q, $^2J_{(C,F)}$ = 293.1 Hz, CF_3COOH), 124.07, 129.90, 144.35, 146.75, 162.8 (q, $^2J_{(C,F)}$ = 35.2 Hz, CF_3COOH), 176.06, 176.62; HRMS (FAB) calculated for $C_{22}H_{36}N_5O_6$, 466.2666 $[M+H]^+$, found: 466.2661 $[M+H]^+$.

Synthesis of 1,8-*N,N′*-Bis-(carboxymethyl)-4-*N″*-(4′-aminophenethyl)-1,4,8,11-tetraaza cyclotetradecane (7·2TFA). To a solution of compound **6** (1.22 g, 1.76 mmol) in water (40 mL) was added 10% Pd/C (0.31 g). The resulting mixture was stirred under H_2 (g) at room temperature for 12 h. The reaction mixture was filtered through a Celite pad which was washed with water (2 × 20 mL). The combined filtrate was evaporated under vacuum to give an oily residue which was triturated with Et_2O to provide an off-white solid **7** (1.15 g, 99% yield). ^{1}H NMR (500 MHz, D_2O, 25 °C): δ = 1.82−2.04 (m, 4H; CH_2), 2.58−2.85 (m, 6H; CH_2), 2.88−3.78 (m, 18H; CH_2), 7.35−7.37 (dd, $^2J_{(H,H)}$ = 10 Hz, 2H; CH), 7.41−7.43 (dd, $^2J_{(H,H)}$ = 10 Hz, 2H; CH); ^{13}C NMR (125.8 MHz, D_2O, 25 °C): δ = 23.66, 25.06, 30.26, 47.37, 50.14, 51.33, 52.61, 53.14, 53.64, 53.96, 56.16, 56.45, 56.71, 58.76, 118.79 (q, $^2J_{(C,F)}$ = 291.9 Hz, CF_3COOH), 125.92, 131.31, 132.90, 139.88, 165.30 (q, $^2J_{(C,F)}$ = 35.2 Hz, CF_3COOH), 178.04, 178.78; HRMS (FAB) calculated for $C_{22}H_{38}N_5O_4$, 436.2924 $[M+H]^+$, found: 436.2925 $[M+H]^+$.

Synthesis of 1,8-*N,N′*-Bis-(carboxymethyl)-4-*N″*-(4′-isothiocyanatophenethyl)-1,4,8,11-tetraazacyclotetradecane (TE2A-Bn-NCS) (8). To a solution of compound **7** (1.05 g, 1.58 mmol) in water (20 mL) was carefully added thiophosgene (**CAUTION!** $CSCl_2$ is considered highly toxic) (3.64 mL, 5.46 g, 47.47 mmol) in $CHCl_3$ (20 mL). The reaction mixture was stirred for 3 h at room temperature and the layers were allowed to separate. The aqueous layer was removed and the organic $CHCl_3$ layer was then washed with water (2 × 50 mL). The combined aqueous layers were washed with $CHCl_3$ (3 × 50 mL) to remove unreacted thiophosgene. Finally, the aqueous layer was lyophilized to afford white solid **8** (0.74 g, 98% yield). ^{1}H NMR (500 MHz, D_2O, 25 °C): δ = 1.94 (s, 4H; CH_2), 2.61−2.94 (m, 6H; CH_2), 2.98−3.62 (m, 18H; CH_2), 7.11−7.12 (dd, $^2J_{(H,H)}$ = 5 Hz, 2H; CH), 7.26−7.27 (dd, $^2J_{(H,H)}$ = 5 Hz, 2H; CH); ^{13}C NMR (125 MHz, D_2O, 25 °C): δ = 23.57, 24.54, 30.72, 46.53, 49.75, 51.48, 52.18, 53.27, 56.64, 56.71, 56.80, 58.21, 128.65, 131.93, 132.69, 136.76, 138.23, 176.95, 177.193; HRMS (FAB) calculated for $C_{23}H_{36}N_5O_4S$, 478.2488 $[M+H]^+$, found: 478.2484 $[M+H]^+$.

Synthesis of Cu-TE2A-Bn-NH$_2$. To a solution of TE2A-Bn-NH_2 **7** (267 mg, 0.40 mmol) and $Cu(ClO_4)_2{\cdot}6H_2O$ (149 mg, 0.40 mmol) in 20 mL of methanol was added 1 M aqueous solution of NaOH (2.41 mL, 2.41 mmol). The resulting clear blue solution was refluxed for 30 min, cooled, and filtered through Celite bed. The filtrate was subjected to diethyl ether diffusion. The deposited blue crystals were collected and dried (178 mg, 89% yield). HRMS (FAB) calculated for $C_{22}H_{36}CuN_5O_4$, 497.2063 $[M+H]^+$, Found: 497.2066 $[M+H]^+$; Elemental Analysis Calcd For $C_{22}H_{35}CuN_5O_4{\cdot}3H_2O$: C 47.94, H 7.50, N 12.71, Found: C 47.99, H 7.35, N 12.69. Visible electronic spectrum: λ_{max} (H_2O)/592 nm (ε = 141 M^{-1} cm^{-1}); λ_{max} (5 M HCl)/566 nm (ε = 169 M^{-1} cm^{-1}). Crystals suitable for X-ray structure determination were grown from a methanol solution upon diethyl ether diffusion.

Acid Decomplexation Studies by Spectrophotometer. Acid decomplexation studies were performed under pseudo first-order conditions using sample concentrations of 3 mmol in 5 M HCl at 50 or 90 °C. Changes in the absorption maxima with time were monitored using a Shimadzu UV−vis spectrophotometer (UV-1650PC) in thermostatted cells. The decreasing absorbance at the λ_{max} of each spectrum (Cu-TE2A-Bn-NH_2 566 nm) was used to monitor the progress of the decomplexation reaction. Half-lives were calculated from the slopes of linear ln(absorbance) vs time plots. Each experiment was repeated two to three times and mean values of half-lives are reported.

Acid Decomplexation Studies by HPLC. Sample concentration of copper complexes (Cu-TE2A-Bn-NH_2, and Cu-TE2A) studied were 3 mmol in 12 M HCl. UV-HPLC spectrum in 12 M HCl at 90 °C was recorded at specific time points by injecting an aliquot (20 μL) onto a reverse phase Xbridge C18 column (4.6 × 150 mm, 5 μm) with an isocratic flow (Cu-TE2A-Bn-NH_2, 0.1% TFA/H_2O:MeOH 94:6, and Cu-TE2A, 30 mM citric acid, 1 mL/min flow rate). The decreasing absorbance at UV region (280 nm) was used to monitor the progress of the decomplexation reaction. The stability of TE2A-Bn-NH_2 itself was also monitored under the same condition (12 M HCl, 90 °C). UV-HPLC spectra were serially recorded by injecting 30 μL aliquot of the chelator into a reverse phase Xbridge C18 column with an isocratic flow (H_2O:acetonitrile (94:6), 1 mL/min flow rate) and the progress of reaction was monitored at UV region (254 nm). UV spectra of TE2A-Bn-NH_2 and Cu-TE2A-Bn-NH_2 (0.3 mM) were measured in 5 M HCl.

Electrochemical Studies. Cyclic voltammetry was conducted with a Biologic model SP-150 with three-electrode configuration. The working electrode was a glassy carbon (diameter = 3 mm), Ag/AgCl (sat. KCl) reference electrode, and Pt wire counter electrode. Samples (1 mM) were run in 0.2 M phosphate buffer adjusted to pH 7.0 with glacial acetic acid at scan rate 100 mV/s. The solutions were deoxygenated for 15 min with Ar prior to use and kept under Ar atmosphere during measurement.

X-ray Crystallography of Cu-TE2A-Bn-NH_2. Single crystal X-ray diffraction data were collected using an Bruker SMART APEX2 ULTRA and a APEX II CCD area detector with a multilayer-monochromated Mo Kα radiation (λ = 0.71073 Å) generated by a rotating anode. Data collection, data reduction, and semiempirical absorption correction were carried out using the software package APEX2. All of the calculations for the structure determination were carried out using the SHELXTL package. All non-H atoms were refined anisotropically. All hydrogen atoms were included in calculated positions with isotropic thermal parameters 1.2 times those of attached atoms.

Radiolabeling of TE2A-Bn-NH_2. Complexation of ^{64}Cu with TE2A-Bn-NH_2 was achieved by a 30-min preincubation of TE2A-Bn-NH_2 (100 μg) in EtOH with an excess of Cs_2CO_3 at 90 °C with constant stirring. Following centrifugation, $^{64}CuCl_2$ was added to the isolated supernatant. The mixture was vortexed and incubated at 90 °C for 30 min. The mixture was centrifuged, and the isolated supernatant was evaporated. The dried mixture was dissolved in water, and passed through the 0.2 μm Nylon Acrodisk 13 filter. Formation of ^{64}Cu-TE2A-Bn-NH_2 complexes was verified by radio-TLC using a mobile phase consisting of MeOH:10% ammonium acetate (1:1) on silica plates. Radio-HPLC analysis of ^{64}Cu-TE2A-Bn-NH_2 was accomplished using Xbridge C18 column (4.6 × 150 mm, 5 μm) with an isocratic method (0.1% TFA in water:MeOH (96:4), 1 mL/min flow rate).

In Vitro Serum Stability of ^{64}Cu-TE2A-Bn-NH_2. In vitro serum stability of ^{64}Cu-TE2A-Bn-NH_2 was carried out by adding 50 μL of ^{64}Cu-TE2A-Bn-NH_2 (1−2 mCi) to 500 μL of FBS (Fetal Bovine Serum). The solution was incubated at 37 °C, and samples were analyzed by radio-TLC at 0, 10, 30, 60 min, and 2, 4, 10, 24, 48, and 72 h postadministration to FBS. Serum stability studies were carried out in duplicate.

Conjugation of TE2A-Bn-NCS to Trastuzumab. Trastuzumab (4 mg) was added to a solution of TE2A-Bn-NCS (0.53 mg) in 0.1 M Na_2CO_3 (pH 9.0, 100 μL). The resulting solution was gently agitated at room temperature overnight. The following day, this solution was placed on a centricon YM-50 (Millipore), and spun down to reduce the volume and washed with PBS (pH 7.4, 2 mL) three times to remove unreacted TE2A-Bn-NCS chelator. The purified TE2A-Bn-NCS-trastuzumab conjugate was collected in 2 mL of PBS and stored at −20 °C.

The conjugation of DOTA-Bn-NCS with trastuzumab was carried out using DOTA-Bn-NCS (0.74 mg) instead of TE2A-Bn-NCS in a similar way to that above.

MALDI-TOF Analysis of Trastuzumab, TE2A-Bn-NCS-Trastuzumab, and DOTA-Bn-NCS-Trastuzumab. Measurement of the level of chelator conjugated to trastuzumab followed the method using the matrix-assisted laser desorption ionization time-of-flight mass spectrometry (MALDI-TOF MS) method (TOF/TOF 5800 System, AB SCIEX). TE2A-Bn-NCS-trastuzumab and DOTA-Bn-NCS-trastuzumab were adjusted to approximately 10−20 picomol/μL of antibody by addition of Q water. A solution of 20 mg/mL sinapinic acid (SIGMA) in 50:50 acetonitrile/0.1% (v/v) trifluoroacetic acid−water was used as the MALDI matrix. After mixing the sample and matrix in 1:1 volume ratio, 2 μL of the mixture was spotted on the target plate and allowed to air-dry prior to mass analysis. The instrument was operated in linear mode for intact proteins. In the experiments, external calibration was applied to the instrument after data collection with data explorer software (AB SCIEX). BSA (SIGMA, $M+H^+$ = 66 431, $2M+H^+$ = 132 861) was used as external calibration for intact proteins. A spectrum was obtained by averaging 600 laser shots using continuous stage motion mode within the sample well. The laser power was adjusted to 5800 fixed intensity. The mass range was applied from 25 kDa to 180 kDa and focus to 150 kDa.

^{64}Cu-Radiolabeling of TE2A-Bn-NCS-Trastuzumab. ^{64}Cu (0.5−2 mCi) in 0.1 M NH_4OAc buffer (pH 8.0, 100 μL) was added to 80 μg of TE2A-Bn-NCS-trastuzumab in 0.1 M NH_4OAc buffer (pH 8.0, 100 μL) or simple distilled water. The reaction mixture was incubated at 25 °C for 10 min, then 50 μg of DTPA was added and the reaction mixture was further incubated for 20 min at 30 °C. The radiochemical yield was checked with instant thin layer chromatography (ITLC-SG, saline). The ^{64}Cu-labeled TE2A-Bn-NCS-trastuzumab was purified by centrifugation using YM-50 filter to remove any ^{64}Cu-DTPA complexes. Radiochemical purity was determined by size exclusion high-performance liquid chromatography (Bio Silect SEC 250-5 300 × 7.8 mm; flow rate 1 mL/min, with the isocratic mobile phase consisting of PBS, pH 7.4).

^{64}Cu-Radiolabeling of DOTA-Bn-NCS-Trastuzumab. ^{64}Cu (1.0−1.2 mCi) in 0.1 M NaOAc buffer (pH 5.5, 100 μL) was added to 80 μg of DOTA-Bn-NCS-trastuzumab in 0.1 M NaOAc buffer (pH 5.5, 100 μL). The reaction mixture was incubated at 40 °C for 60 min, then 50 μg DTPA was added and the reaction mixture was further incubated for 20 min at 30 °C. The ^{64}Cu-labeled DOTA-Bn-NCS-trastuzumab was also purified by centrifugation using YM-50 to remove any free ^{64}Cu ions. The radiochemical yield and purity was determined as above in TE2A-Bn-NCS-trastuzumab.

Specific Activity Determination of ^{64}Cu-TE2A-Bn-NCS-Trastuzumab and ^{64}Cu-DOTA-Bn-NCS-Trastuzumab. The fixed amount of ^{64}Cu (220 μCi) in 0.1 M NH_4OAc buffer (pH 8.0, 100 μL) was added to various concentrations (1−80 μg) of TE2A-Bn-NCS-trastuzumab in 0.1 M NH_4OAc buffer (pH 8.0, 100 μL). The reaction mixture was incubated at 25 °C for 10 min, then 50 μg of DTPA was added and the reaction mixture was further incubated for 20 min at 30 °C. The radiochemical yield was checked with instant thin layer chromatography (ITLC-SG, saline). Three concentrations of TE2A-Bn-NCS-trastuzumab showing 40−90% radiolabeling yield was chosen to calculate the specific activity of ^{64}Cu-labeled TE2A-Bn-NCS-trastuzumab (9.0 ± 0.39 μCi/μg). The specific activity of ^{64}Cu-DOTA-Bn-NCS-trastuzumab (8.5 ± 0.48 μCi/μg) was also measured in the same way except using the radiolabeling condition of DOTA-Bn-NCS-trastuzumab (0.1 M NaOAc buffer (pH 5.5), 40 °C, 60 min).

Animal Models. All animal experiments were conducted in compliance with the Animal Care and Use Committee requirements of Kyungpook National University. Xenograft tumor models of NIH3T6.7 cell lines were prepared using 6-week-old BALB/c nu/nu female nude mice. 5×106 NIH3T6.7 cells were inoculated subcutaneously into left shoulder and right flank of mice. Tumors of appropriate size usually grew within 15 d after the implantation.

Biodistribution of ^{64}Cu-TE2A-Bn-NCS-Trastuzumab and ^{64}Cu-DOTA-Bn-NCS-Trastuzumab. The NIH3T6.7 tumor-bearing BALB/c nude mice (n = 4) were injected via tail-vein with ^{64}Cu-TE2A-Bn-NCS-trastuzumab and ^{64}Cu-DOTA-Bn-NCS-trastuzumab (ca. 20 μCi in 200 μL saline per mouse) for comparison studies. Animals were sacrificed at 1 and 2 days postinjection. Organs and tissues of interest (blood,

muscle, bone, spleen, kidney, intestine, liver, and tumor) were removed, weighed, and counted using gamma-counter. The percent of injected dose per gram (%ID/g) was calculated by comparison to a weighted, counted standard.

MicroPET Imaging in NIH3T6.7 Tumor Bearing Nude Mice. Small animal PET scans and image analysis were performed using a microPET R4 rodent model scanner. Imaging studies were carried out on female nude mice bearing NIH3T6.7 tumors. The mice were injected via the tail vein with ^{64}Cu-TE2A-Bn-NCS-trastuzumab (200 μCi). At 1, 2, and 3 days after injection, the mice were anesthetized with 1% to 2% isoflurane, positioned in prone position, and imaged. The images were reconstructed by a two-dimensional ordered-subsets expectation maximum (OSEM) algorithm, and no correction was necessary for attenuation or scatter correction.

RESULTS AND DISCUSSION

Synthesis of Bifunctional Chelator TE2A-Bn-NCS. New TE2A-Bn-NCS was successfully synthesized in seven steps from commercially available cyclam as shown in Scheme 1. First, two

Scheme 1. Seven-Step Synthesis of TE2A-Bn-NCS from Cyclam

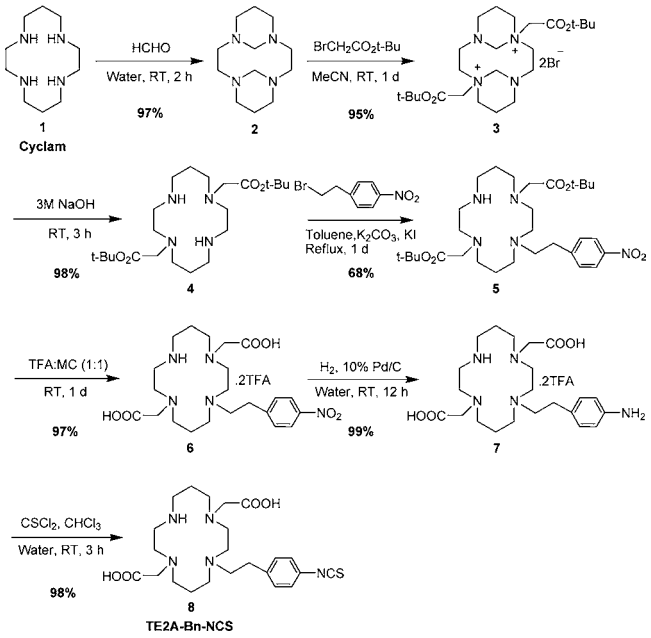

acetate groups were regioselectively introduced at 1,8-positioned amines of cyclam using the protection/alkylation/deprotection strategy as reported previously.[39] Briefly, four amines of cyclam were protected by formaldehyde followed by alkylation of *tert*-butyl bromoacetate, which give trans-disubstituted cyclam compound (**3**). Only methylene bridges on adjacent amines were deprotected by treatment of 3 M NaOH at room temperature. The *tert*-butyl ester groups of **3** were not broken by strong base at this stage thanks to insolubility of **4** in aqueous solution. Next, the second functional group needed for easy conjugation with biomolecules was introduced on one of the two regenerated secondary amine groups. A mixture of disubstituted cyclam (**4**) and 3 equiv of 4-nitro phenylethyl bromide was refluxed in the presence of anhydrous K_2CO_3 and KI. After workup, the residue was purified via column chromatography to afford pure **5** as an oil. Even though excess alkylating agent was used, only trisubstituted cyclam compound (**5**) was obtained as the major product. Deprotection of the *tert*-butyl ester groups of **5** was carried out by the treatment of trifluoroacetic acid to give pure white solid (**6**). For the reduction of NO_2 to NH_2 group, compound **6** was treated with 10% Pd/C in water under H_2 (g) at room temperature. The NH_2 group of **7** was converted to NCS group by treating it with highly excess thiophosgene (**CAUTION!** $CSCl_2$ is considered highly toxic) to afford the final product TE2A-Bn-NCS (**8**). During NCS conversion reaction, the TFA salts of intermediate **7** were gone and TFA salt-free TE2A-Bn-NCS was obtained. When the reduction step of nitro group proceeded before the deprotection of *tert*-butyl groups, higher amounts of TFA salts were found in intermediate **7** and the next NCS conversion reaction did not proceed cleanly. Proton and carbon NMR spectra matched well with the expected peak patterns of TE2A-Bn-NCS (Figure 2). No TFA peaks were observed in ^{13}C NMR spectrum. All other intermediates were also fully characterized by ^{1}H and ^{13}C NMR and HR-Mass spectroscopy (see Supporting Information).

By designing an efficient synthetic route, all of the intermediates and products except **5** were isolated in quantitative yield without tedious column purification. The total reaction time was 4 days and the overall yield from commercially available cyclam reached 57%. This synthesis time and yield are far superior in comparison with previously reported similar BFCs such as DOTA-Bn-NCS,[22,40] TETA-Bn-NCS,[23,41,42] and NOTA-Bn-NCS,[12,43] in which an extra functional group (NCS) is attached on macrocyclic ring carbon atom. Their typical total reaction time and overall yield from starting compounds were over 14 days and less than 5%, respectively (Table 1). In the current synthesis, the extra functional group was simply introduced on the secondary amine group of cyclam, which could avoid low-yielding cyclization steps in other BFC syntheses. Even though the intra- and intercondensation between NCS group and secondary amines of TE2A-Bn-NCS was worried before synthesis, we did not observe any noticeable thiourea bond formation during synthesis and storage of TE2A-Bn-NCS.

Synthesis of Cu-TE2A-Bn-NH$_2$ (Cu-7). To evaluate the kinetic stability of copper(II) complex, which is known to be more important than their thermodynamic stabilities in physiological conditions, we synthesized Cu(II) complex of TE2A-Bn-NH_2 (**7**) as model compound because NCS group of TE2A-Bn-NCS seemed to be involved in Cu(II) complex formation, and the expected Cu complex, in which Cu(II) ions are hexa-coordinated with four nitrogens of tetraazamacrocycle and two acetic acid groups, was not isolated. Cu complex of TE2A-Bn-NH_2 was easily synthesized by treating TE2A-Bn-NH_2 with $Cu(ClO_4)_2{\cdot}6H_2O$ in 1 M NaOH in reflux condition. The Cu-TE2A-Bn-NH_2 complex was recrystallized from methanol layer by slow diffusion of diethyl ether in 89% yield.

Acid Decomplexation and Electrochemical Studies. Even though we had proven previously that TE2A could form much more stable Cu(II) complex compared to TETA, the effect of introduction of an extra functional group on one of two secondary amines was evaluated by acid decomplexation and electrochemical study. The half-lives for the acid-assisted decomplexation of Cu-TE2A-Bn-NH_2 and Cu-TE2A complexes and the reduction potentials of copper(II) complexes are summarized in Table 2. Acid-assisted decomplexation of the Cu(II) complex is a good barometer in estimating the in vivo stability of complexes.[44] The half-life of Cu-TE2A-Bn-NH_2

dx.doi.org/10.1021/bc400192a | Bioconjugate Chem. 2013, 24, 1356−1366

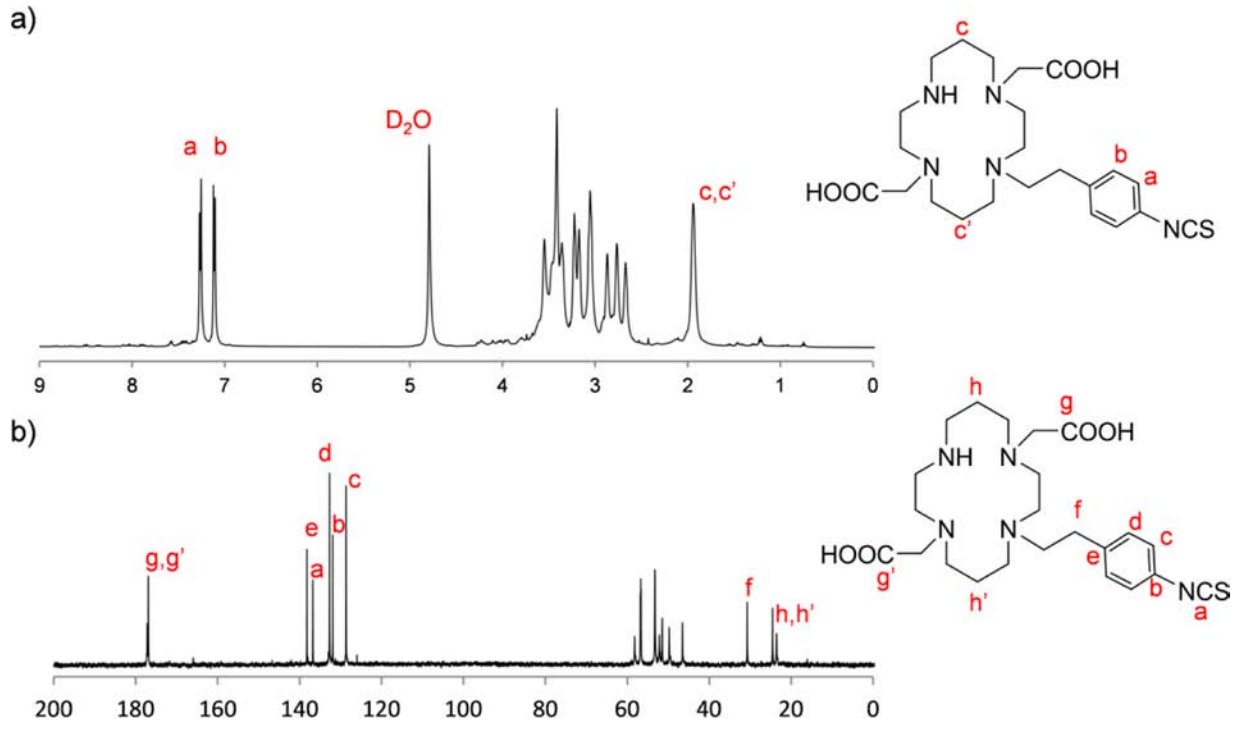

Figure 2. ^{1}H (a) and ^{13}C (b) NMR spectra of TE2A-Bn-NCS with several peak assignments.

Table 1. Comparison of Total Synthesis Time and Overall Yield from Starting Compounds

bifunctional chelator	total number of synthesis steps	total reaction time for synthesis	overall yield
TE2A-Bn-NCS	7	4 days	57%
NOTA-Bn-NCS	12	14 days	2.9%
DOTA-Bn-NCS	10	21 days	3.6%
TETA-Bn-NCS	10	30 days	3.3%

Table 2. Half-Lives[a] for Acid Decomplexation under Pseudo First Order Conditions at 5 M HCl Concentration and Reduction Potentials of Cu(II) Complexes

complex	5 M HCl, 50 °C	5 M HCl, 90 °C	E_{red} (V) vs Ag/AgCl (0.2 M phosphate)
Cu-TE2A-Bn-NH_2	261.9(7) h	84.7(4) m	−1.02 (irrev)
Cu-TE2A	92.6(2) h	46.2(8) m	−1.04 (irrev)

[a]Half-lives are mean values of 2−3 experiments.

complex in 5 M HCl at 50 °C was 261.9 h, which was almost 3 times higher than the value of 92.6 h for Cu-TE2A in the same condition. In 5 M HCl at 90 °C, the half-life of Cu-TE2A-Bn-NH_2 complex was dramatically reduced to 84.7 min, but still it was almost double compared to the value of 46.2 min for Cu-TE2A.

To check the Cu complex stability in harsher conditions and to monitor degradation patterns, Cu-TE2A-Bn-NH_2 and Cu-TE2A complexes were tested in 12 M HCl at 90 °C and degradation pattern was monitored by HPLC (Figure 3a and b). More than 60% of intact Cu-TE2A-Bn-NH_2 remained after 30 min heating and took 4 h to reduce to 1%, whereas about 90% of Cu-TE2A was decomposed at 30 min and only 1% of intact Cu-TE2A remained at 50 min postheating. All these acid decomplexation studies showed that Cu-TE2A-Bn-NH_2 is more kinetically stable than Cu-TE2A in at least as strong acidic conditions. Higher stability of Cu-TE2A-Bn-NH_2 could be attributed to the extra one alkylation on secondary amine of cyclam.[45] As a control experiment, the stability of TE2A-Bn-NH_2 itself was also monitored in the same harsh acidic conditions (12 M HCl, 90 °C). It did not show any sign of decomposition up to 4 h (see Supporting Information, Figure S3). However, because the UV absorbance of TE2A-Bn-NH_2 in the absence of Cu was 70 times lower than that of Cu-TE2A-Bn-NH_2 at 280 nm (Figure S1), the contribution of UV absorbance of Cu-released chelator to overall UV absorbance at monitoring wavelength should be minimal.

Owing to the different preferences of coordination pattern of Cu(I) ion from Cu(II), the reduction of the Cu(II) complex to Cu(I) leads to the breakdown of the Cu(II) complex.[44] The electrochemical behaviors of Cu-TE2A-Bn-NH_2 and Cu-TE2A were examined by cyclic voltammetry studies (Figure 3c and d). The two cyclic voltammograms were almost undistinguishable. Both the Cu-TE2A-Bn-NH_2 and Cu-TE2A complexes showed irreversible reduction voltammograms with reduction potential of −1.02 V and −1.04 V (vs Ag/AgCl), respectively. These cyclic voltammetry studies showed that the effect of one more alkylation on the electrochemical behavior of Cu(II) complex is minimal.[46]

X-ray Crystallography of Cu-TE2A-Bn-NH_2. Recrystallization of Cu-TE2A-Bn-NH_2 in methanol/ether solvent system produced a single crystal suitable for X-ray analysis. The core coordination sphere around the Cu(II) ion adapts slightly distorted octahedral geometry, in which the copper atom is strongly coordinated by four macrocyclic nitrogens in equatorial positions to attain a strong ligand field in the plane of the ring [Cu−N 2.038(1), 2.055(1), 2.067(1), 2.101(1) Å] and the two carboxylate oxygen atoms occupy the elongated axial positions [Cu−O 2.290(1), 2.326(1) Å] (Figure 4). The

dx.doi.org/10.1021/bc400192a | Bioconjugate Chem. 2013, 24, 1356−1366

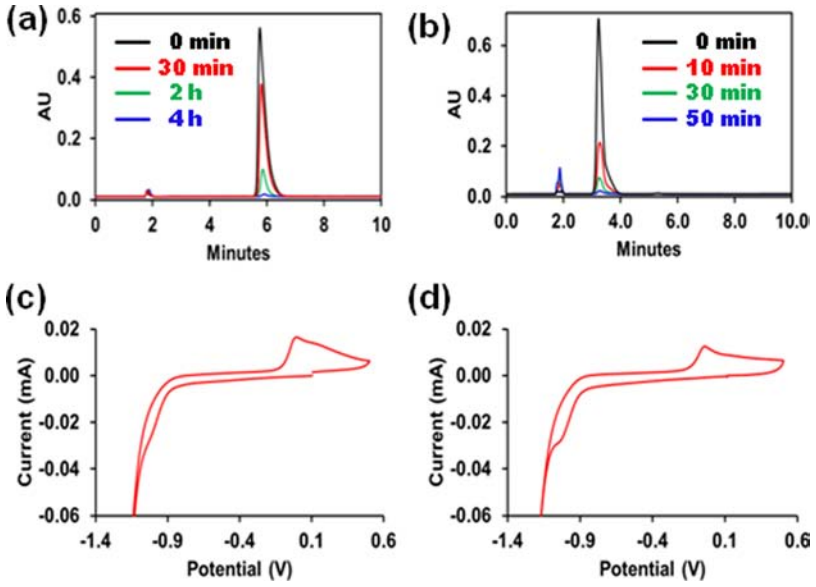

Figure 3. Time-dependent UV-HPLC chromatograms of Cu-TE2A-Bn-NH_2 (a) and Cu-TE2A (b) during acidic decomplexation in 12 M HCl at 90 °C. Cyclic voltammograms (scan rate 100 mV/s, 0.2 M phosphate buffer, pH 7) of Cu-TE2A-Bn-NH_2 (c) and Cu-TE2A (d).

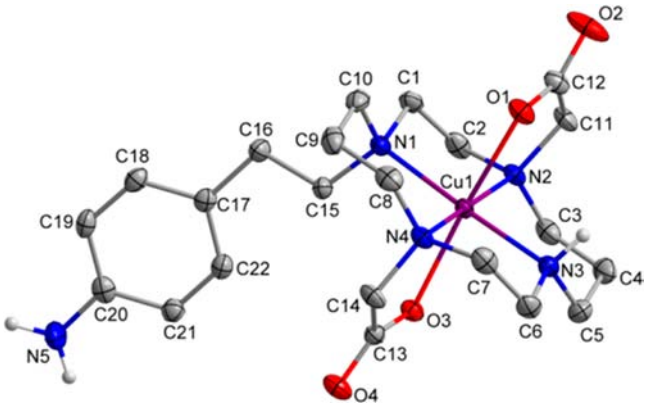

Figure 4. X-ray structure of the Cu-TE2A-Bn-NH_2 complex with hydrogens omitted for clarity.

pendant $CH_2CH_2PhNH_2$ group in Cu-TE2A-Bn-NH_2 is located far away from the copper coordination center. Except for that, the core coordination geometry is virtually the same as that of Cu-TE2A.[47] The X-ray structure clearly showed that one more *N*-substitution on TE2A does not disrupt the strong N_4 in-plain ligand field, thus allowing Cu-TE2A-Bn-NH_2 to attain high kinetic inertness and thermodynamic stability. Detailed X-ray crystallographic data is available in Supporting Information.

Conjugation and ^{64}Cu Radiolabeling. After confirming the high in vitro stability of the Cu(II) complex of new BFC, we tested its conjugation feasibility and radiolabeling efficiency with ^{64}Cu. Trastuzumab, the first FDA approved monoclonal antibody for immunotherapy, was chosen as a model antibody for conjugation. Trastuzumab is known to selectively target the HER2 protein and block its overexpression.[48] TE2A-Bn-NCS was conjugated smoothly with trastuzumab by forming strong thiourea bonds by the reaction of NCS group of TE2A-Bn-NCS and lysine NH_2 group of antibody (Scheme 2). The

Scheme 2. Conjugation of TE2A-Bn-NCS with Trastuzumab and ^{64}Cu-Radiolabeling

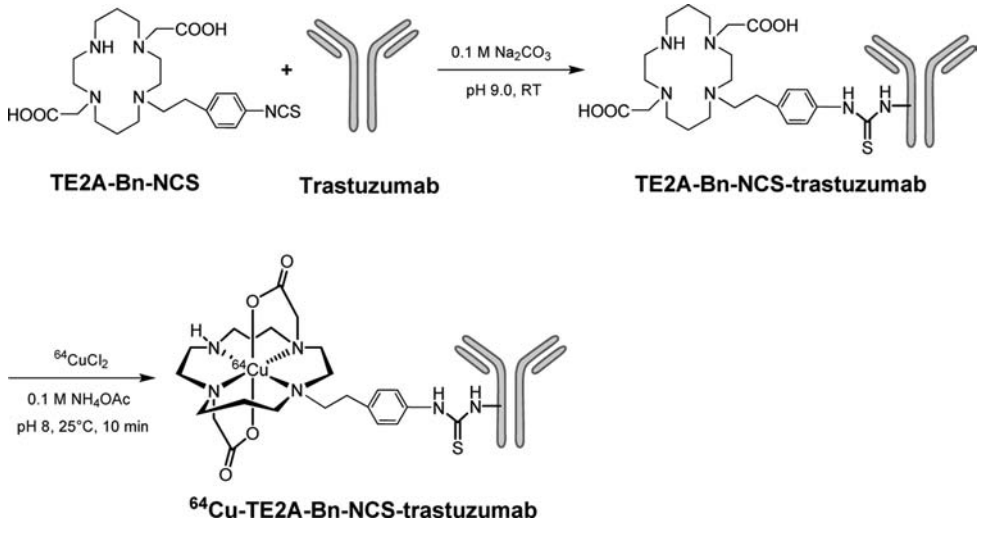

dx.doi.org/10.1021/bc400192a | *Bioconjugate Chem.* 2013, 24, 1356−1366

TE2A-Bn-NCS-trastuzumab conjugate was purified by simple centrifugal filtration (Ultracel YM-50, Millipore) and collected in PBS buffer. The purified TE2A-Bn-NCS-trastuzumab conjugate was analyzed by size-exclusion HPLC [Bio Sil SEC 250 (Bio-Rad, USA), PBS (pH 7.4), 1 mL/min] (Figure 5, top)

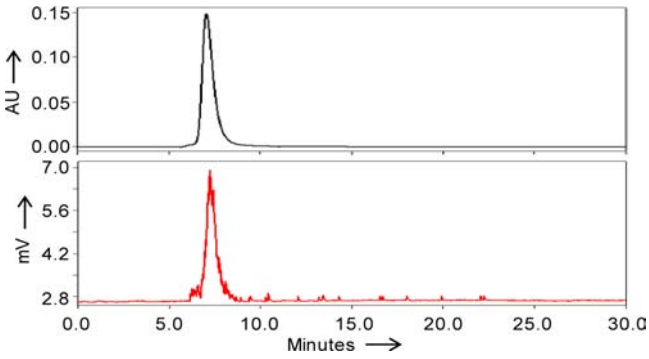

Figure 5. UV-HPLC chromatogram (280 nm) of TE2A-Bn-NCS-trastuzumab (top) compared with radio-HPLC chromatogram of ^{64}Cu-TE2A-Bn-NCS-trastuzumab (bottom).

and was characterized by MALTI-TOF mass spectroscopy (Figure 6). The number of chelator, TE2A-Bn-NCS, on each

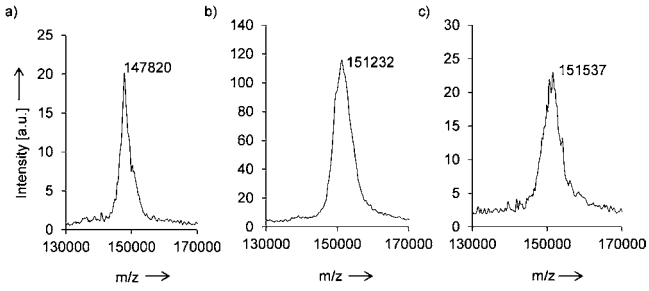

Figure 6. MALDI-TOF characterization of trastuzumab (a), TE2A-Bn-NCS-trastuzumab (b), and DOTA-Bn-NCS-trastuzumab (c).

trastuzumab was calculated by the mass difference observed in mass analysis of trastuzumab and TE2A-Bn-NCS-trastuzumab (147820 and 151232, respectively). A difference of 3412 mass unit was observed, which corresponds to an average of 7.1 TE2A-Bn-NCS molecules per antibody.

The purified TE2A-Bn-NCS-trastuzumab conjugate was radiolabeled quantitatively by incubation with $^{64}CuCl_2$ in 0.1 M NH_4OAc buffer (pH 8.0) or simple distilled water at 25 °C for 10 min (Scheme 2). More than 90% of radiolabeling yield was measured even after 1 min of incubation. After centrifugal removal of trace amount of free ^{64}Cu(II) ions by excess DTPA complexation, the radiochemical purity of ^{64}Cu-TE2A-Bn-NCS-trastuzumab reached 100% (Figure 5, bottom). Until now, various antibodies have been radiolabeled via several DOTA and TETA-based BFCs. However, their typical labeling conditions require at least 30−60 min of incubation at 35−43 °C to give 60−95% radiolabeling yield.[11,12,15,22,48] In contrast, TE2A-Bn-NCS-conjugated antibody showed instant quantitative radiolabeling yield at room temperature, which are highly required conditions for the successful radiolabeling of heat- and radiation-sensitive antibody.

For the comparison of in vivo stability and biodistribution behavior, DOTA-Bn-NCS-trastuzumab was also prepared in a similar manner as TE2A-Bn-NCS and the number of chelators, DOTA-Bn-NCS, per trastuzumab was calculated to be 6.7 by MALDI-TOF analysis (Figure 6). About 90% radiolabeling yield was achieved after 1 h incubation of DOTA-Bn-NCS-trastuzumab with ^{64}Cu ions at 40 °C,[22] and unlabeled free ^{64}Cu ions were removed by the competitive DTPA complexation followed by centrifugal purification, resulting in 100% pure ^{64}Cu-DOTA-Bn-NCS-trastuzumab. When exactly the same radiolabeling condition of TE2A-Bn-NCS-trastuzumab was used, the labeling yield of DOTA-Bn-NCS-trastuzumab with ^{64}Cu was less than 10%. After purification, the specific activity of ^{64}Cu-labeled TE2A-Bn-NCS-trastuzumab and DOTA-Bn-NCS-trastuzumab was calculated to be 9.0 ± 0.39 μCi/μg and 8.5 ± 0.48 μCi/μg, respectively.

Radiolabeling of TE2A-Bn-NH_2 and in Vitro Serum Stability of ^{64}Cu-TE2A-Bn-NH_2. Radiolabeling of TE2A-Bn-NH_2 was carried out by using the Cs_2CO_3 method to achieve quantitative radiolabeling yield and the desired radio complex was obtained in 100% radiochemical purity by HPLC separation. The radiolabeled ^{64}Cu-TE2A-Bn-NH_2 did not show any noticeable degradation at 37 °C in fetal bovine serum up to 3 days (see Supporting Information, Figure S4).

Biodistribution Studies. The in vivo stability and targeting affinity of prepared ^{64}Cu-TE2A-Bn-NCS-trastuzumab were examined by biodistribution studies in Her2/neu positive tumor models and compared with ^{64}Cu-DOTA-Bn-NCS-trastuzumab (Figure 7). The highest uptake of ^{64}Cu-TE2A-

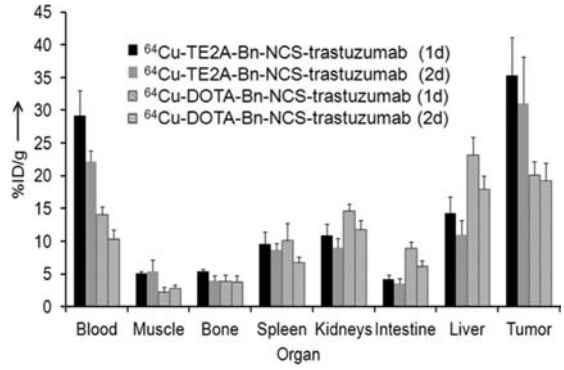

Figure 7. Biodistribution data of ^{64}Cu-TE2A-Bn-NCS-trastuzumab and ^{64}Cu-DOTA-Bn-NCS-trastuzumab at 1 and 2 d postinjection in NIH3T6.7 tumor bearing nude mice (n = 4).

Bn-NCS-trastuzumab was found in tumors at both 1 and 2 d. The activity in tumor at 1 d (35.3 ± 5.8%ID/g) was slightly decreased at 2 d (31.1 ± 7.1%ID/g). High activity retention was also shown in blood at 1 d but slowly decreased until 2 d (29.2 ± 3.7 and 22.2 ± 1.6, respectively), which reflects long circulation behavior of trastuzumab antibody in the blood.[12] The liver, kidney, and spleen showed the next highest activity uptakes. The biodistribution pattern of ^{64}Cu-DOTA-Bn-NCS-trastuzumab was distinctively different from that of ^{64}Cu-TE2A-Bn-NCS-trastuzumab even though only BFCs were different in two conjugates. First of all, ^{64}Cu-DOTA-Bn-NCS-trastuzumab showed much faster blood clearance. The activity in blood was less than 50% compared to the TE2A analog at both 1 and 2 d (14.0 ± 1.2 and 10.4 ± 1.3%ID/g, respectively), which is still comparable to the reported blood uptakes of DOTA-conjugated trastuzumab.[22,49] However, liver and kidney activities of ^{64}Cu-DOTA-Bn-NCS-trastuzumab were even higher than those of ^{64}Cu-TE2A-Bn-NCS-trastuzumab at both time points. Considering the long blood half-life of intact

dx.doi.org/10.1021/bc400192a | Bioconjugate Chem. 2013, 24, 1356−1366

antibodies, all these data suggest that free ^{64}Cu ions are dissociated from the trastuzumab-conjugated DOTA complex and bind to the copper binding protein, then remained in these organs with retarded clearance.[12] Consequently, less tumor uptake of ^{64}Cu-DOTA-Bn-NCS-trastuzumab was observed at both 1 d (20.1 ± 2.0%ID/g) and 2 d (19.2 ± 2.6%ID/g), which is only 57% and 62% of the corresponding values of the TE2A analog, respectively.

MicroPET Imaging Studies. Finally a ^{64}Cu-immuno-PET imaging study was carried out to monitor the in vivo behavior of ^{64}Cu-TE2A-Bn-NCS-trastuzumab noninvasively in real time (Figure 8). By considering long blood circulation of intact

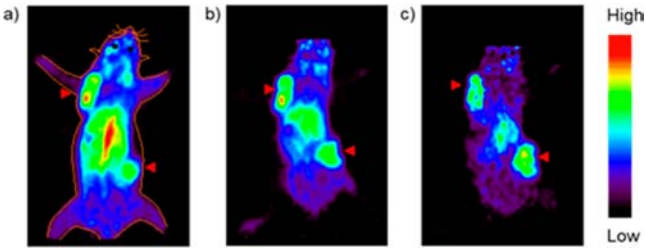

Figure 8. MicroPET images of female nude mice bearing NIH3T6.7 tumors at 1 (a), 2 (b), and 3 d (c) after injection of ^{64}Cu-TE2A-Bn-NCS-trastuzumab.

antibodies, NIH3T6.7 tumor-bearing mice were imaged on a daily basis up to 3 days after tail vein injection of ^{64}Cu-TE2A-Bn-NCS-trastuzumab (200 μCi). At 1 d postinjection, high uptakes were found in both tumors and internal organs. Even though one tumor in the left shoulder was easily recognized, the other tumor in the right flank close to the internal organs did not show a clear margin of the tumor because of high activity in the liver and kidneys. However, the activity of background, including blood and internal organs, decreased gradually at 2 and 3 d, while tumor activity decreased in lower amounts compared to others. As a result, both of the two Her2/neu positive tumors could be unambiguously assigned at 2 d, and even more clearly visualized with a higher tumor-to-background ratio at 3 d. These microPET studies clearly demonstrated that ^{64}Cu-labeled antibody could be easily monitored up to 3 days by immuno-PET imaging when antibody was radiolabeled firmly using appropriate BFC such as TE2A-Bn-NCS.

CONCLUSION

In conclusion, a new tetraazamacrocyclic BFC, in which two acetic acid group and an extra NCS pendant arm are substitued on N-atoms of cyclam for strong Cu(II) complexation and easy conjugation with antibody, respectively, was synthesized in high yield. A newly synthesized TE2A-Bn-NCS showed many promising physical properties as a BFC such as facile conjugation with antibody, high stability of formed Cu(II) complex, instant radiolabeling at room temperature, reduced demetalation of free ^{64}Cu ions in physiological conditions, and vivid tumor imaging with low background noise. All these data strongly suggest that TE2A-Bn-NCS has great potential as a BFC for ^{64}Cu-immuno-PET imaging.

ASSOCIATED CONTENT

Supporting Information

Characterization of compounds (**4**–**8**), characterization of Cu-TE2A-Bn-NH$_2$, UV spectra of chelator and Cu complex, acid decomplexation study by spectrophotometer, X-ray crystallographic data of Cu-TE2A-Bn-NH$_2$, serum stability. CCDC 902630 contains the supplementary crystallographic data for this paper. This material is available free of charge via the Internet at http://pubs.acs.org.

AUTHOR INFORMATION

Corresponding Author

*Fax: +82-53-426-4944, Tel: +82-53-420-4947, E-mail: yooj@knu.ac.kr.

Author Contributions

Darpan N. Pandya and Nikunj Bhatt contributed equally.

Notes

The authors declare no competing financial interest.

ACKNOWLEDGMENTS

This work was supported by the National Research Foundation of Korea (NRF) grant funded by the Korea government (MSIP) (No. 20090081817, 2012-0006386, 20090078235, 2013R1A2A2A01012250). The Korea Basic Science Institute (Daegu) is acknowledged for the NMR and HR-Mass measurements. We thank Dr. Seo Jong Bok (Seoul Center, KBSI) for the MALDI-TOF analysis.

REFERENCES

(1) Steiner, M., and Neri, D. (2011) Antibody-radionuclide conjugates for cancer therapy: historical considerations and new trends. *Clin. Cancer Res. 17*, 6406–6416.

(2) Wu, A. M. (2009) Antibodies and antimatter: the resurgence of immuno-PET. *J. Nucl. Med. 50*, 2–5.

(3) Kaur, S., Venktaraman, G., Jain, M., Senapati, S., Garg, P. K., and Batra, S. K. (2012) Recent trends in antibody-based oncologic imaging. *Cancer Lett. 315*, 97–111.

(4) Chamarthy, M. R., Williams, S. C., and Moadel, R. M. (2011) Radioimmunotherapy of non-Hodgkin's lymphoma: from the 'magic bullets' to 'radioactive magic bullets'. *Yale J. Biol. Med. 84*, 391–407.

(5) Lee, F. T. (2003) Immuno-PET for tumor targeting. *J. Nucl. Med. 44*, 1282–1283.

(6) Vugts, D. J., and van Dongen, G. A. M. S. (2011) ^{89}Zr-labeled compounds for PET imaging guided personalized therapy. *Drug Discovery Today: Technol. 8*, e53–e61.

(7) Knowles Scott, M., and Wu Anna, M. (2012) Advances in immuno-positron emission tomography: antibodies for molecular imaging in oncology. *J. Clin. Oncol. 30*, 3884–3892.

(8) van Dongen, G. A. M. S., Visser, G. W. M., Lub-de Hooge, M. N., de Vries, E. G., and Perk, L. R. (2007) Immuno-PET: a navigator in monoclonal antibody development and applications. *Oncologist 12*, 1379–1389.

(9) Shokeen, M., and Anderson, C. J. (2009) Molecular imaging of cancer with copper-64 radiopharmaceuticals and positron emission tomography (PET). *Acc. Chem. Res. 42*, 832–841.

(10) Kume, M., Carey, P. C., Gaehle, G., Madrid, E., Voller, T., Margenau, W., Welch, M. J., and Lapi, S. E. (2012) A semi-automated system for the routine production of copper-64. *Appl. Radiat. Isot. 70*, 1803–1806.

(11) Cai, W., Chen, K., He, L., Cao, Q., Koong, A., and Chen, X. (2007) Quantitative PET of EGFR expression in xenograft-bearing mice using ^{64}Cu-labeled cetuximab, a chimeric anti-EGFR monoclonal antibody. *Eur. J. Nucl. Med. Mol. Imaging 34*, 850–858.

(12) Zhang, Y., Hong, H., Engle, J. W., Bean, J., Yang, Y., Leigh, B. R., Barnhart, T. E., and Cai, W. (2011) Positron emission tomography imaging of CD105 expression with a ^{64}Cu-labeled monoclonal antibody: NOTA is superior to DOTA. *PloS One 6*, e28005.

(13) Anderson, C. J., Connett, J. M., Schwarz, S. W., Rocque, P. A., Guo, L. W., Philpott, G. W., Zinn, K. R., Meares, C. F., and Welch, M.

J. (1992) Copper-64-labeled antibodies for PET imaging. *J. Nucl. Med. 33*, 1685−1691.
(14) Anderson, C. J., and Ferdani, R. (2009) Copper-64 radiopharmaceuticals for PET imaging of cancer: advances in preclinical and clinical research. *Cancer Biother. Radiopharm. 24*, 379−393.
(15) Lewis, M. R., Kao, J. Y., Anderson, A. L., Shively, J. E., and Raubitschek, A. (2001) An improved method for conjugating monoclonal antibodies with N-hydroxysulfosuccinimidyl DOTA. *Bioconjugate Chem. 12*, 320−324.
(16) Chan, C., Scollard, D. A., McLarty, K., Smith, S., and Reilly, R. M. (2011) A comparison of ^{111}In- or ^{64}Cu-DOTA-trastuzumab Fab fragments for imaging subcutaneous HER2-positive tumor xenografts in athymic mice using microSPECT/CT or microPET/CT. *EJNMMI Res. 1*, 15.
(17) Lewis, M. R., Boswell, C. A., Laforest, R., Buettner, T. L., Ye, D., Connett, J. M., and Anderson, C. J. (2001) Conjugation of monoclonal antibodies with TETA using activated esters: biological comparison of ^{64}Cu-TETA-1A3 with ^{64}Cu-BAT-2IT-1A3. *Cancer Biother. Radiopharm. 16*, 483−494.
(18) Moi, M. K., Meares, C. F., McCall, M. J., Cole, W. C., and DeNardo, S. J. (1985) Copper chelates as probes of biological systems: stable copper complexes with a macrocyclic bifunctional chelating agent. *Anal. Biochem. 148*, 249−253.
(19) Bass, L. A., Wang, M., Welch, M. J., and Anderson, C. J. (2000) In vivo transchelation of copper-64 from TETA-octreotide to superoxide dismutase in rat liver. *Bioconjugate Chem. 11*, 527−532.
(20) Boswell, C. A., Sun, X., Niu, W., Weisman, G. R., Wong, E. H., Rheingold, A. L., and Anderson, C. J. (2004) Comparative in vivo stability of copper-64-labeled cross-bridged and conventional tetraazamacrocyclic complexes. *J. Med. Chem. 47*, 1465−1474.
(21) Sampath, L., Kwon, S., Hall, M. A., Price, R. E., and Sevick-Muraca, E. M. (2010) Detection of cancer metastases with a dual-labeled near-infrared/positron emission tomography imaging agent. *Transl. Oncol. 3*, 307−317.
(22) Ferreira, C. L., Yapp, D. T., Crisp, S., Sutherland, B. W., Ng, S. S., Gleave, M., Bensimon, C., Jurek, P., and Kiefer, G. E. (2010) Comparison of bifunctional chelates for ^{64}Cu antibody imaging. *Eur. J. Nucl. Med. Mol. Imaging 37*, 2117−2126.
(23) Rogers, B. E., Anderson, C. J., Connett, J. M., Guo, L. W., Edwards, W. B., Sherman, E. L., Zinn, K. R., and Welch, M. J. (1996) Comparison of four bifunctional chelates for radiolabeling monoclonal antibodies with copper radioisotopes: biodistribution and metabolism. *Bioconjugate Chem. 7*, 511−522.
(24) Zimmermann, K., Grunberg, J., Honer, M., Ametamey, S., Schubiger, P. A., and Novak-Hofer, I. (2003) Targeting of renal carcinoma with $^{67/64}$Cu-labeled anti-L1-CAM antibody chCE7: selection of copper ligands and PET imaging. *Nucl. Med. Biol. 30*, 417−427.
(25) Wadas, T. J., Eiblmaier, M., Zheleznyak, A., Sherman, C. D., Ferdani, R., Liang, K., Achilefu, S., and Anderson, C. J. (2008) Preparation and biological evaluation of ^{64}Cu-CB-TE2A-sst2-ANT, a somatostatin antagonist for PET imaging of somatostatin receptor-positive tumors. *J. Nucl. Med. 49*, 1819−1827.
(26) Anderson, C. J., Wadas, T. J., Wong, E. H., and Weisman, G. R. (2008) Cross-bridged macrocyclic chelators for stable complexation of copper radionuclides for PET imaging. *Q. J. Nucl. Med. Mol. Imaging 52*, 185−192.
(27) Jiang, M., Ferdani, R., Shokeen, M., and Anderson, C. J. (2013) Comparison of two cross-bridged macrocyclic chelators for the evaluation of ^{64}Cu-labeled-LLP2A, a peptidomimetic ligand targeting VLA-4-positive tumors. *Nucl. Med. Biol. 40*, 245−251.
(28) Guo, Y., Ferdani, R., and Anderson, C. J. (2012) Preparation and biological evaluation of ^{64}Cu labeled Tyr3-octreotate using a phosphonic acid-based cross-bridged macrocyclic chelator. *Bioconjugate Chem. 23*, 1470−1477.
(29) Pandya, D. N., Kim, J. Y., Park, J. C., Lee, H., Phapale, P. B., Kwak, W., Choi, T. H., Cheon, G. J., Yoon, Y.-R., and Yoo, J. (2010) Revival of TE2A; a better chelate for Cu(II) ions than TETA? *Chem. Commun. 46*, 3517−3519.
(30) Pandya, D. N., Kim, J. Y., Kwak, W., Park, J. C., Gawande, M. B., An, G. I., Ryu, E. K., and Yoo, J. (2010) A new synthesis of TE2A as a potential bifunctional chelator for ^{64}Cu. *Nucl. Med. Mol. Imaging 44*, 185−192.
(31) Sprague, J. E., Peng, Y., Fiamengo, A. L., Woodin, K. S., Southwick, E. A., Weisman, G. R., Wong, E. H., Golen, J. A., Rheingold, A. L., and Anderson, C. J. (2007) Synthesis, characterization and in vivo studies of Cu(II)-64-labeled cross-bridged tetraazamacrocycle-amide complexes as models of peptide conjugate imaging agents. *J. Med. Chem. 50*, 2527−2535.
(32) Jones-Wilson, T. M., Deal, K. A., Anderson, C. J., McCarthy, D. W., Kovacs, Z., Motekaitis, R. J., Sherry, A. D., Martell, A. E., and Welch, M. J. (1998) The in vivo behavior of copper-64-labeled azamacrocyclic complexes. *Nucl. Med. Biol. 25*, 523−530.
(33) Yoo, J., Reichert, D. E., and Welch, M. J. (2004) Comparative in vivo behavior studies of cyclen-based copper-64 complexes: regioselective synthesis, X-ray structure, radiochemistry, log P, and biodistribution. *J. Med. Chem. 47*, 6625−6637.
(34) Harris, M. (2004) Monoclonal antibodies as therapeutic agents for cancer. *Lancet Oncol. 5*, 292−302.
(35) Pegram, M., and Liao, J. (2012) Trastuzumab treatment in multiple lines: current data and future directions. *Clin. Breast Cancer 12*, 10−18.
(36) Kang, H. S., Huh, Y. M., Kim, S., and Lee, D.-k. (2009) Isolation of RNA aptamers targeting HER-2-overexpressing breast cancer cells using cell-SELEX. *Bull. Korean Chem. Soc. 30*, 1827−1831.
(37) Lee, J. H., Huh, Y. M., Jun, Y. W., Seo, J. W., Jang, J. T., Song, H. T., Kim, S., Cho, E. J., Yoon, H. G., Suh, J. S., and Cheon, J. (2007) Artificially engineered magnetic nanoparticles for ultra-sensitive molecular imaging. *Nat. Med. 13*, 95−99.
(38) Yang, J., Lee, C.-H., Ko, H.-J., Suh, J.-S., Yoon, H.-G., Lee, K., Huh, Y.-M., and Haam, S. (2007) Multifunctional magneto-polymeric nanohybrids for targeted detection and synergistic therapeutic effects on breast cancer. *Angew. Chem., Int. Ed. 46*, 8836−8839.
(39) Pandya, D. N., Dale, A. V., Kim, J. Y., Lee, H., Ha, Y. S., An, G. I., and Yoo, J. (2012) New macrobicyclic chelator for the development of ultrastable ^{64}Cu-radiolabeled bioconjugate. *Bioconjugate Chem. 23*, 330−335.
(40) Yoshida, C., Tsuji, A. B., Sudo, H., Sugyo, A., Sogawa, C., Inubushi, M., Uehara, T., Fukumura, T., Koizumi, M., Arano, Y., and Saga, T. (2011) Development of positron emission tomography probe of ^{64}Cu-labeled anti-C-kit 12A8 Fab to measure protooncogene C-kit expression. *Nucl. Med. Biol. 38*, 331−337.
(41) McMurry, T. J., Brechbiel, M., Kumar, K., and Gansow, O. A. (1992) Convenient synthesis of bifunctional tetraaza macrocycles. *Bioconjugate Chem. 3*, 108−117.
(42) Brechbiel, M. W., Gansow, O. A., Atcher, R. W., Schlom, J., Esteban, J., Simpson, D., and Colcher, D. (1986) Synthesis of 1-(p-isothiocyanatobenzyl) derivatives of DTPA and EDTA. Antibody labeling and tumor-imaging studies. *Inorg. Chem. 25*, 2772−2781.
(43) McMurry, T. J., Brechbiel, M., Wu, C., and Gansow, O. A. (1993) Synthesis of 2-(p-thiocyanatobenzyl)-1,4,7-triazacyclononane-1,4,7-triacetic acid: Application of the 4-methoxy-2,3,6-trimethylbenzenesulfonamide protecting group in the synthesis of macrocyclic polyamines. *Bioconjugate Chem. 4*, 236−245.
(44) Woodin, K. S., Heroux, K. J., Boswell, C. A., Wong, E. H., Weisman, G. R., Niu, W., Tomellini, S. A., Anderson, C. J., Zakharov, L. N., and Rheingold, A. L. (2005) Kinetic inertness and electrochemical behavior of copper(II) tetraazamacrocyclic complexes: possible implications for in vivo stability. *Eur. J. Inorg. Chem. 2005*, 4829−4833.
(45) Kotek, J., Lubal, P., Hermann, P., Cisarova, I., Lukes, I., Godula, T., Svobodova, I., Taborsky, P., and Havel, J. (2003) High thermodynamic stability and extraordinary kinetic inertness of copper(II) complexes with 1,4,8,11-tetraazacyclotetradecane-1,8-bis-(methylphosphonic acid): example of a rare isomerism between

kinetically inert penta- and hexacoordinated copper(II) complexes. *Chem.—Eur. J. 9*, 233−248.
(46) Dong, Y., Lawrance, G. A., Lindoy, L. F., and Turner, P. (2003) Macrocyclic ligand design. Interaction of a series of successively N-benzylated derivatives of 1,4,8,11-tetraazacyclotetradecane (cyclam) with copper(II) and nickel(II). *Dalton Trans.*, 1567−1576.
(47) Chapman, J., Ferguson, G., Gallagher, J. F., Jennings, M. C., and Parker, D. (1992) Copper and nickel complexes of 1,8-disubstituted derivatives of 1,4,8,11-tetraazacyclotetradecane. *J. Chem. Soc., Dalton Trans.*, 345−353.
(48) Paudyal, P., Paudyal, B., Hanaoka, H., Oriuchi, N., Iida, Y., Yoshioka, H., Tominaga, H., Watanabe, S., Ishioka, N. S., and Endo, K. (2010) Imaging and biodistribution of Her2/neu expression in non-small cell lung cancer xenografts with Cu-labeled trastuzumab PET. *Cancer Sci. 101*, 1045−1050.
(49) Niu, G., Li, Z., Cao, Q., and Chen, X. (2009) Monitoring therapeutic response of human ovarian cancer to 17-DMAG by noninvasive PET imaging with ^{64}Cu-DOTA-trastuzumab. *Eur. J. Nucl. Med. Mol. Imaging 36*, 1510−1519.